THE JOURNAL OF PHYSICAL CHEMISTRY A LETTERS

2009, *113,* 4844–4848
Published on Web 03/30/2009

Anion-Catalyzed Dissolution of NO_2 on Aqueous Microdroplets

A. Yabushita,[†] S. Enami,[‡] Y. Sakamoto,[†] M. Kawasaki,[†] M. R. Hoffmann,[‡] and A. J. Colussi*,[‡]

Department of Molecular Engineering, Kyoto University, Kyoto 615-8510, Japan, and W. M. Keck Laboratories, California Institute of Technology, Pasadena, California 91125

Received: January 23, 2009; Revised Manuscript Received: March 19, 2009

Fifty-seven years after NO_x ($NO + NO_2$) were identified as essential components of photochemical smog, atmospheric chemical models fail to correctly predict $\bullet OH/HO_2\bullet$ concentrations under NO_x-rich conditions. This deficiency is due, in part, to the uncertain rates and mechanism for the reactive dissolution of $NO_2(g)$ ($2NO_2 + H_2O = NO_3^- + H^+ + HONO$) in fog and aerosol droplets. Thus, state-of-the-art models parametrize the uptake of NO_2 by atmospheric aerosol from data obtained on "deactivated tunnel wall residue". Here, we report experiments in which NO_3^- production on the surface of microdroplets exposed to $NO_2(g)$ for ~1 ms is monitored by online thermospray mass spectrometry. NO_2 does not dissolve in deionized water (NO_3^- signals below the detection limit) but readily produces NO_3^- on aqueous NaX (X = Cl, Br, I) microdroplets with NO_2 uptake coefficients γ that vary nonmonotonically with electrolyte concentration and peak at $\gamma_{max} \sim 10^{-4}$ for [NaX] ~ 1 mM, which is $>10^3$ larger than that in neat water. Since I^- is partially oxidized to $I_2^{\bullet-}$ in this process, anions seem to capture $NO_2(g)$ into $X{-}NO_2^{\bullet-}$ radical anions for further reaction at the air/water interface. By showing that γ is strongly enhanced by electrolytes, these results resolve outstanding discrepancies between previous measurements in neat water versus NaCl-seeded clouds. They also provide a general mechanism for the heterogeneous conversion of $NO_2(g)$ to ($NO_3^- + HONO$) on the surface of aqueous media.

Nitrogen dioxide (NO_2), the pollutant that imparts its brownish hue to urban skies, is produced by photooxidation of the nitric oxide (NO) emitted by high-temperature combustion sources (Scheme 1).[1] In the gas phase, NO_2 is photolyzed to ($O + NO$) during the daytime and oxidized to NO_3 at night.[2] However, NO_2 also disproportionates into nitric and nitrous acids on cloud and fog droplets via reaction 1[3−6]

$$2NO_2(g) + H_2O(l) \rightarrow HONO(g) + NO_3^-(aq) + H^+(aq) \quad (1)$$

$$HONO(g) + h\nu\ (\lambda < 405\ nm) \rightarrow NO + \bullet OH \quad (2)$$

Photochemical smog is particularly sensitive to reaction 1, which launches a pathway that converts NO_2 into •OH, the most reactive atmospheric intermediate, at longer wavelengths and higher solar zenith angles than the conventional route via O_3 photolysis (see Scheme 1).[7−11] Recently, measurements based on improved detection techniques revealed unexpectedly high HONO daytime concentrations, which would require reaction 1 to proceed >60 times faster at noon than at nighttime.[4,12,13] This finding evokes the lingering discrepancies between observed and under/overestimated $\bullet OH/HO_2\bullet$ concentrations in atmospheres containing >100 pptv NO_x[10,14−17] and revives unsolved issues about reaction 1.[18]

Predictions that reaction 1, the bimolecular disproportionation of a sparingly water-soluble gas, should be exceedingly slow on clouds and fogs because it is so on pure water,[19−21] were not confirmed in the field or the laboratory.[3,22] $NO_2(g)$ uptake coefficients on "water" range from $\gamma < 10^{-7}$ up to $\sim 10^{-3}$ and are independent (rather than linearly dependent) of $[NO_2(g)]$.[3,19,23−28] Although the second-order disproportionation of $NO_2(aq)$ in bulk water is not assisted even by strong nucleophiles,[29] its heterogeneous uptake is significantly enhanced by various solutes, particularly by reducing ones,[30] such as amines, sulfite, or iodide.[5,31,32] This apparent anomaly suggests that the mechanism of reaction 1 at the air/water interface may be different from that in bulk solution. Few techniques, however, can instantly monitor the formation of products without further processing, under essentially wall-less conditions, on the surface of fresh microdroplets exposed to ppmv $NO_2(g)$ levels at atmospheric pressure for less than ~1 ms.

We investigated reaction 1 on microdroplets generated by pneumatic nebulization of aqueous electrolyte solutions into ppmv $NO_2(g)/N_2$ mixtures at atmospheric pressure. Solutions are injected into the spraying chamber of an electrospray mass spectrometer through a grounded stainless steel nozzle issuing nebulizer N_2 gas (see Figure S1 in Supporting Information). The high-velocity nebulizer gas breaks up the liquid jet into micrometer-size droplets carrying excess charges of either sign.[33] The negatively charged microdroplets generated in this process carry modest excess charges,[33] in contrast with those produced in conventional electrospray sources maintained at high voltage relative to ground.[34,35] Microdroplets rapidly evaporate solvent

* To whom correspondence should be addressed. E-mail: ajcoluss@caltech.edu.
[†] Kyoto University.
[‡] California Institute of Technology.

10.1021/jp900685f CCC: $40.75

SCHEME 1: Photochemical Smog Cycles[a]

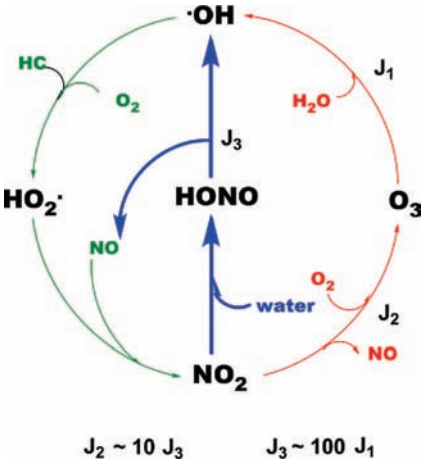

[a] J_1, J_2, and J_3 are the first-order rate constants (in time^{-1}) for the solar photolysis of O_3, NO_2, and HONO, respectively. HC stands for reactive hydrocarbons, and "water" represents fog or cloud droplets.

in the dry N_2(g) emanating from the electrically polarized inlet to the mass spectrometer while being drawn to it with increasing acceleration, $a = (ze/m)E$, because the electric field E becomes more intense in its vicinity and because they rapidly lose mass m while keeping their excess charges ze. The spraying chamber is not, therefore, a conventional well-stirred reactor with a normal distribution of microdroplet residence times but a unidirectional flow reactor which shrinking microdroplets traverse at exponentially increasing speeds (and shorter residence times). The strong direct correlation between residence time and droplet size, in addition to the perpendicular crossing of the spray with the NO_2(g) plume, ensures that NO_2(g) mostly interacts with nascent microdroplets (see Figure S1, Supporting Information). Solvent evaporation leads to charge crowding, whereby droplets shed their interfacial films carrying (from electrostatics) the excess charges into smaller offspring.[36] These events ultimately produce nanodroplets from which bare ions are electrostatically ejected into the gas phase.[34,37,38] Given the orthogonal configuration of the instrument, mass spectra report on gas-phase ions sampled from the periphery of the spray cone rather than from its axis, along which the bulk of the liquid advances (Figure S1, Supporting Information).[39] Thus, these experiments probe, within 1 ms, the ion composition of the interfacial layers (see below) of nascent microdroplets that had just reacted with NO_2(g). Further details can be found in previous publications from our laboratory (see also Supporting Information for further details).[40−43]

Negative ion mass spectra ($m/z \geq 50$) of deionized water (pH 7.0) microdroplets nebulized into a chamber continuously flushed with NO_2(g) are verifiably and consistently featureless, that is, mass spectral signals are within noise levels (background trace in Figure 1A). This result (1) excludes detectable levels of HNO_3 impurities in our NO_2(g)/N_2 mixtures, (2) precludes artifactual NO_3^- production in our instrument, and (3) provides direct evidence that the negative excess interfacial charges carried by our droplets are insufficient to trap NO_2(g) in significant amounts (see below). Strong NO_3^- signals (m/z = 62), however, develop on aqueous NaOH microdroplets above pH ∼ 10. Since the aerial surfaces of aqueous electrolyte solutions as a rule are negatively charged relative to the bulk, that is, anions approach the interface closer than cations,[44,45] this finding actually implies that OH^- is able to catalyze the disproportionation of NO_2(g) into (NO_2^- + NO_3^-) at the

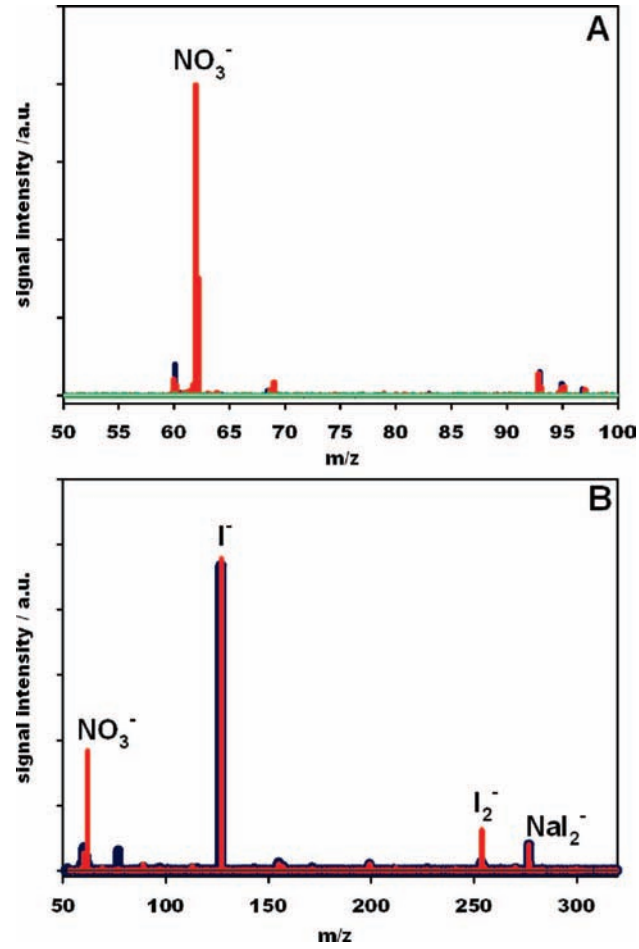

Figure 1. Anion-catalyzed nitrate formation on aqueous microdroplets. (A) Thermospray mass spectra (TSMS) of pure water at pH ∼ 7 in the presence of 8.0 ppmv NO_2(g) (green) and of 1 mM NaCl droplets at pH ∼ 7 in the absence (blue)/presence (red) of 0.7 ppmv NO_2(g). (B) TSMS of 1 mM NaI droplets at pH ∼ 7 in the absence (blue)/presence (red) of 0.4 ppmv NO_2(g). One ppmv ≡ 2.4 × 10^{13} molecules cm^{-3} at 1 atm and 300 K.

interface[29] and prompted us to explore the possibility that other anions X^- could also promote reaction 1.

Figure 1A also shows the mass spectrum acquired from 1 mM NaCl microdroplets at pH 7.0 sprayed into NO_2(g)/N_2 under identical conditions. New, sizable m/z = 62 signals are observed that can be ascribed to NO_3^- as the exclusive anion product in the $m/z \geq 50$ mass range accessible to our instrument. Similar results were obtained with NaBr, NaF, and $NaHSO_4$ solutions (see Figure S2, Supporting Information) without detectable Br^-, F^- or HSO_4^- losses, confirming that reaction 1 undergoes general base catalysis.[46] Although NO_2^- (m/z = 46) lies below the instrumental mass threshold, it should have been possible to detect it as its cluster $Na(NO_2)_2^-$ (m/z = 115) had NO_2^- and NO_3^- been present at similar (>2 mM) concentrations at the air/water interface (see Figure S3, Supporting Information). The absence of detectable m/z = 115 signals therefore implies that neutral HONO (pK_a = 3.37) is quantitatively released (whereas $HONO_2$, pK_a = −1.64, is not) to the gas phase. It should be emphasized that the oxidation of NO_2 to NO_3^- under present strictly anoxic conditions can only occur via NO_2 disproportionation (reaction 1). We verified that NO_3^- signal intensities increase linearly with [NO_2(g)] in the presence of electrolytes (Figure S4, Supporting Information) (see below).

Figure 2 shows [NO_3^-] versus [NaX] data at various NO_2(g) concentrations in the range of 0.01 ≤ [NaX]/mM ≤ 100 for X

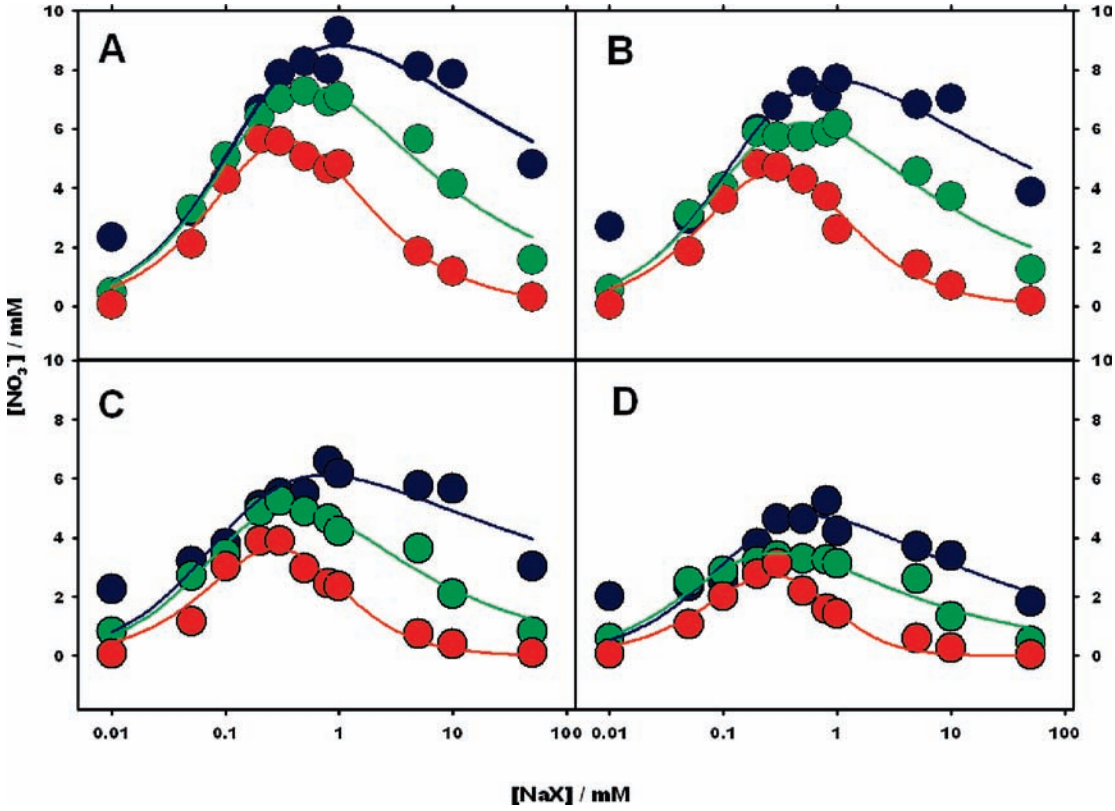

Figure 2. Anion-dependent efficiency of the $NO_2(g) \rightarrow NO_3^-$ conversion on aqueous electrolyte microdroplets. $[NO_3^-]$ versus [NaX] at pH ~ 7; X = Cl (blue), Br (green) and I (red) at (A) $[NO_2(g)] = 7.2 \times 10^{14}$ molecules cm^{-3}, (B) $[NO_2(g)] = 4.8 \times 10^{14}$ molecules cm^{-3}, (C) $[NO_2(g)] = 2.4 \times 10^{14}$ molecules cm^{-3}, and (D) $[NO_2(g)] = 1.2 \times 10^{14}$ molecules cm^{-3}. Solid curves are best fits based on eq 3. $[NO_3^-]$ is calculated from a ($m/z = 62$) signal intensity versus $[NaNO_3]$ calibration plot. See text for details.

$\equiv$ Cl, Br, and I. The curves correspond to best fits based on three- parameter (α; β; Γ) expressions given by

$$[NO_3^-] = \Gamma\vartheta(1 - \vartheta)^\beta \qquad \vartheta = \frac{[X^-]}{\alpha + [X^-]} \tag{3}$$

where ϑ is the anion interfacial fractional coverage, α is the reciprocal of the partitioning coefficient of X^- to the interface, β gauges the attenuation of NO_3^- signals by excess X^-, and Γ is a factor that converts surface coverages in measured $[NO_3^-]$ values. Independent calibrations show that anion signal intensities are directly proportional to bulk concentrations $[X^-]$ but generally plateau above $[X^-] \sim 10$ mM under present conditions (Figure S3, Supporting Information). The gentle (i.e., $0.4 > \beta > 0.1$) decline of NO_3^- signals beyond peak values therefore implies that excess X^- competes with NO_3^- for the air/water interface, thereby attenuating $m/z = 62$ signals. The preceding observations are accounted for by the following mechanism

$$X^- + NO_2(g) \xrightarrow{\text{slow}} [X{-}NO_2^{\bullet -}]_{\text{interface}} \tag{4}$$

$$[X{-}NO_2^{\bullet -}]_{\text{interface}} + NO_2(g) + H_2O \xrightarrow{\text{fast}}$$

$$X^- + HONO + NO_3^- + H^+ \tag{5}$$

The reality of $X{-}NO_2^{\bullet -}$ intermediates having finite lifetimes at the interface is confirmed by experiments on 1 mM NaI microdroplets. In this case, the detection of $I_2^{\bullet -}$ ($m/z = 254$) (Figure 1B) in yields that level off above $[NO_2(g)] \sim 3$ ppmv (Figure S5, Supporting Information) indicates that $I{-}NO_2^{\bullet -}$ undergoes intramolecular electron transfer, $I^-{-}NO_2 \rightarrow I\bullet + NO_2^-$ (followed by $I\bullet + I^- \rightarrow I_2^{\bullet -}$), in competition with reaction 5 at the interface. Given the exceedingly small sticking probability of $NO_2(g)$ on pure water (see below), only at the interface could a second $NO_2(g)$ molecule be rapidly captured by $I{-}NO_2^{\bullet -}$ intermediates.

Mass balance and the stoichiometry of reaction 1 require that

$$\delta[NO_3^-] = \frac{1}{8}\gamma c\tau[NO_2(g)] \tag{6}$$

where δ is the average thickness of the interfacial layers in which NO_3^- is generated and detected, $\gamma([NaX])$ is the $NO_2(g)$ uptake coefficient, $c = 3.72 \times 10^4$ cm s^{-1} is the average $NO_2(g)$ molecular speed at 300 K, and $\tau = 1$ ms is the average $NO_2(g)$/microdroplets contact time. In Figure 2D, $[NO_3^-]_{max} = 4.72$ mM $= 2.83 \times 10^{18}$ ions cm^{-3} were generated at the interface of [NaCl] = 0.62 mM droplets exposed to 1.2×10^{14} $NO_2(g)$ molecules cm^{-3}. Hence, $\gamma_{max} \sim 5.1$ [δ(cm)/τ(s)]. A lower value $\gamma_{max} > 2.6 \times 10^{-4}$ can then be obtained by assuming realistic $\delta \geq 5 \times 10^{-8}$ cm, $\tau \leq 1$ ms bounds. Considering that the detection limit for NO_3^- is <0.1 μM under present conditions, the failure to detect $m/z = 62$ signals on pure water droplets further implies that $\gamma_{water} < 2 \times 10^{-8}$, in accord with previously reported $NO_2(g)$ uptake coefficients on water nanofilms.[23] These estimates are robust because the ratio of $m/z = 62$ signal intensities measured on 1 mM NaCl ($I_{m/z=62}$) and neat water microdroplets ($I^0_{m/z=62}$ $\leq 2 \times$ baseline average signal intensity) under 14 ppmv $NO_2(g)$

SCHEME 2

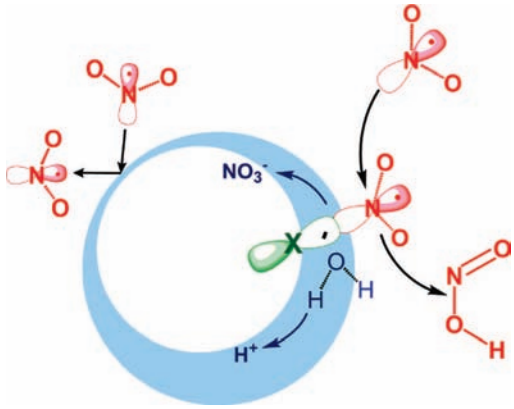

yields $\gamma_{max}/\gamma_{water} = (I_{m/z=62}/I^0_{m/z=62}) \geq 5.6 \times 10^4$. These results rationalize the similar NO_2(g) dissolution rates measured in pure water by the Berkeley and Brookhaven teams[19,28] versus the much larger values determined on clouds consisting of ~3 mM NaCl droplets,[25] in which NO_2(g) uptake is controlled by reaction 4. From Figure 2, uptake coefficients determined on wet/dry seasalt,[47] or concentrated (5.3 M) NaCl aerosols,[24] are expected to be somewhat smaller than the present $\gamma_{max} > 2.6 \times 10^{-4}$ value.

The exceedingly low probability of reaction 1 on pure water is consistent with MD calculations showing that the hydrophobic free radical NO_2 has strong propensity for the surface of neutral clusters $NO_2(H_2O)_n$.[48] Figure 2 shows that the catalytic efficiency of halide anions ($Cl^- > Br^- > I^-$) in reaction 1 follows neither nucleophilicity nor interfacial affinity trends[29,44] but tracks reported $X-NO^{\bullet -}$ bond energies, BDE ($X-NO^{\bullet -}$) = 34.7, 17.2, 14.2, and 11.3 kJ mol^{-1} ($X \equiv F^-, Cl^-, Br^-, I^-$, respectively).[49] Since BDE($X-NO_2^{\bullet -}$)'s are expected to be similarly ordered, we infer that anions capture the 17 electron π-radical NO_2(g) at the air/water interface via charge transfer into its semioccupied molecular orbital[50] rather than by catalyzing NO_2(aq) disproportionation in the bulk phase (Scheme 2).

Maximum rates of NO_2(g) reactive dissolution in clouds and fogs consisting of aqueous electrolyte droplets can be calculated from $R_d = k_d[NO_2(g)]$, $k_d = 0.25\gamma c(S/V)$, where S/V is the total droplet surface per volume of air. Typical S/V values vary between $\sim 2 \times 10^{-5}$ cm^{-1} in clear weather and $\sim 5 \times 10^{-5}$ cm^{-1} during foggy events.[3,18,51] Total electrolyte concentrations of typical cloud and fog droplets naturally display wide variability spanning the 0.1−3 mM range.[52] Thus, from $\gamma_{max} \sim 2 \times 10^{-4}$, one could estimate $k_{d,max} \sim 5 \times 10^{-5}$ s^{-1}, that is, maximum ~ 20% NO_2(g) hourly conversions in clear day conditions, which encompass recent HONO daytime field measurements in Mediterranean urban areas.[53] Note that smaller γ's $< \gamma_{max}$ would account for the diurnal $NO_2 \rightarrow$ HONO conversion rates required by most field studies.[7,23,51,54]

Real cloud and fog droplets are not, however, aqueous solutions of simple electrolytes but also contain a wide array of hydrophilic, hydrophobic, and amphiphilic organic substances that could enhance or inhibit in various ways the NO_2(g) hydrolytic disproportionation rates calculated above.[55,56] The nonmonotonic dependence of γ on [X^-] suggests that the relative humidity and the level of pollution could indeed impact NO_2(g) uptake by atmospheric particles.[8,51,57,58] This phenomenon alone could modulate γ during the day, but we decline to elaborate further at this time. We only wish to emphasize that the presence of electrolytes alone greatly enhances NO_2(g) uptake relative to pure water, rendering alternative proposals, such as the photosensitized reduction of NO_2(g) on aerosolized humic matter,[4,59−61] less relevant. The uncertainties surrounding this issue are highligthed by the fact that the most recent chemical models parametrize the heterogeneous production of HONO in air masses downwind from metropolitan areas using NO_2(g) uptake data obtained on "deactivated tunnel wall residues".[10,62]

Since $J_3 \sim 100J_1$, Scheme 1 shows that under hazy/foggy conditions, that is, at high humidity and reduced insolation, the "HONO cycle" might overtake the "O_3 cycle" producing "smog without ozone".[7] A more efficient HONO cycle than that previously assumed likely underlies the larger discrepancies between observed and predicted HO_x ($\bullet OH + HO_2\bullet$) at higher NO_x levels and high solar zenith angles.[14] Direct $\bullet OH$ production from electronically excited NO_2 (+ H_2O) may also contribute to this phenomenon.[63]

Summing up, anions catalyze the heterogeneous disproportionation of NO_2(g) on cloud and fog droplets by capturing it at the air/water interface. NO_2(g) uptake coefficients are enhanced several orders of magnitude by increasing electrolyte concentration in the sub-millimolar range, peaking at $\gamma_{max} \sim 2 \times 10^{-4}$ values that provide for the elevated, and heretofore unaccounted for, NO_2(g) diurnal conversion rates (1−30% h^{-1}) reported in the literature. Our results provide a benchmark upper bound for the probability of reaction 1 on dilute aqueous microdroplets. NO_2 uptake on actual cloud/fog/aerosol droplets will depend, of course, on their overall makeup. Time-dependent ionic compositions of clouds and fogs are henceforth required to model these processes.

Acknowledgment. We thank Y. Kanaya for helpful discussions. S.E. is grateful to the JSPS research fellowship for young scientists. This project was supported by the National Science Foundation (ATM-0534990) and a grant-in-aid from the Ministry of Education and Science of Japan.

Supporting Information Available: Additional data, data analysis, and experimental details. This material is available free of charge via the Internet at http://pubs.acs.org.

References and Notes

(1) Haagen-Smit, A. J. *Ind. Eng. Chem.* **1952**, *44*, 1342.
(2) Finlayson-Pitts, B. J.; Pitts, J. N. *Chemistry of the Upper and Lower Atmosphere*: Academic Press: San Diego, CA, 2000.
(3) Notholt, J.; Hjorth, J.; Raes, F. *Atmos. Environ.* **1992**, *26A*, 211.
(4) Kleffmann, J. *ChemPhysChem* **2007**, *8*, 1137.
(5) Finlayson-Pitts, B. J.; et al. *Phys. Chem. Chem. Phys.* **2003**, *5*, 223.
(6) Ramazan, K. A.; et al. *J. Phys. Chem. A* **2006**, *110*, 6886.
(7) Acker, K.; et al. *Atmos. Environ.* **2006**, *40*, 3123.
(8) Alicke, B.; Platt, U.; Stutz, J. *J. Geophys. Res., [Atmos.]* **2002**, *107*, DOI: 10.1029/2000JD000075.
(9) Perner, D.; Platt, U. *Geophys. Res. Lett.* **1979**, *6*, 917.
(10) Emmerson, K. M.; et al. *Atmos. Chem. Phys.* **2007**, *7*, 167.
(11) Calvert, J. G.; Yarwood, G.; Dunker, A. M. *Res. Chem. Intermed.* **1994**, *20*, 463.
(12) Acker, K.; Beysens, D.; Moller, D. *Atmos. Res.* **2008**, *87*, 200.
(13) Kleffmann, J.; et al. *Atmos. Environ.* **2006**, *40*, 3640.
(14) Olson, J. R.; et al. *J. Geophys. Res., [Atmos.]* **2006**, *111*, DOI: 10.1029/2005JD006617.
(15) Faloona, I.; et al. *J. Geophys. Res., [Atmos.]* **2000**, *105*, 3771.
(16) Kanaya, Y.; et al. *J. Geophys. Res., [Atmos.]* **2007**, *112*, DOI: 10.1029/2007JD008670.
(17) Kanaya, Y.; et al. *J. Geophys. Res., [Atmos.]* **2008**, *113*, DOI: 10.1029/2007JD008671.
(18) Aumont, B.; Chervier, F.; Laval, S. *Atmos. Environ.* **2003**, *37*, 487.
(19) Schwartz, S. E.; Lee, Y. N. *Atmos. Environ.* **1995**, *29*, 2557.
(20) Schwartz, S. E.; White, W. H. *Trace Atmospheric Constituents*; Wiley: New York, 1983.
(21) Lee, Y. N.; Schwartz, S. E. *J. Geophys. Res., [Atmos.]* **1981**, *86*, 1971.

(22) Lammel, G.; Cape, J. N. *Chem. Soc. Rev.* **1996**, *25*, 361.
(23) Kleffmann, J.; Becker, K. H.; Wiesen, P. *Atmos. Environ.* **1998**, *32*, 2721.
(24) Abbatt, J. P. D.; Waschewsky, G. C. G. *J. Phys. Chem. A* **1998**, *102*, 3719.
(25) Bambauer, A.; Brantner, B.; Paige, M.; Novakov, T. *Atmos. Environ.* **1994**, *28*, 3225.
(26) Cheung, J. L.; et al. *J. Phys. Chem. A* **2000**, *104*, 2655.
(27) Harrison, R. M.; Collins, G. M. *J. Atmos. Chem.* **1998**, *30*, 397.
(28) Novakov, T. *Atmos. Environ.* **1995**, *29*, 2559.
(29) Becker, R. H.; Nicoson, J. S.; Margerum, D. W. *Inorg. Chem.* **2003**, *42*, 7938.
(30) Huie, R. E. *Toxicology* **1994**, *89*, 193.
(31) Nash, T. *J. Chem. Soc. A* **1970**, 3023.
(32) Weis, D. D.; Ewing, G. E. *J. Phys. Chem. A* **1999**, *103*, 4865.
(33) Zilch, L. W.; et al. *J. Phys. Chem. A* **2008**, *112*, 13352.
(34) Manisali, I.; Chen, D. D. Y.; Schneider, B. B. *TrAC, Trends Anal. Chem.* **2006**, *25*, 243.
(35) Hirabayashi, A.; Sakairi, M.; Koizumi, H. *Anal. Chem.* **1995**, *67*, 2878.
(36) Kebarle, P.; Peschke, M. *Anal. Chim. Acta* **2000**, *406*, 11.
(37) Iribarne, J. V.; Dziedzic, P. J.; Thomson, B. A. *Int. J. Mass Spectrom. Ion Process.* **1983**, *50*, 331.
(38) Nguyen, S.; Fenn, J. B. *Proc. Natl. Acad. Sci. U.S.A.* **2007**, *104*, 1111.
(39) Tang, K. Q.; Smith, R. D. *J. Am. Soc. Mass Spectrom.* **2001**, *12*, 343.
(40) Enami, S.; Hoffmann, M. R.; Colussi, A. J. *Proc. Natl. Acad. Sci. U.S.A.* **2008**, *105*, 7365.
(41) Enami, S.; et al. *J. Phys. Chem. A* **2007**, *111*, 8749.
(42) Enami, S.; et al. *J. Phys. Chem. A* **2007**, *111*, 13032.
(43) Enami, S.; et al. *Chem. Phys. Lett.* **2008**, *455*, 316.
(44) Cheng, J.; Vecitis, C.; Hoffmann, M. R.; Colussi, A. J. *J. Phys. Chem. B* **2006**, *110*, 25598.
(45) Cheng, J.; Hoffmann, M. R.; Colussi, A. J. *J. Phys. Chem. B* **2008**, *112*, 7157.
(46) Lowry, T. H.; Schueller Richardson, K. *Mechanism and Theory in Organic Chemistry*, 3rd ed.; Harper & Row: New York, 1987.
(47) Karlsson, R.; Ljungstrom, E. *J. Aerosol. Sci.* **1995**, *26*, 39.
(48) Bezrukov, D. S.; Novakovskaya, Y. V. *Struct. Chem.* **2004**, *15*, 77.
(49) Hiraoka, K.; et al. *Chem. Phys. Lett.* **2000**, *323*, 155.
(50) Wan, J. K. S.; Pitts, J. N.; Beichert, P.; Finlayson-Pitts, B. J. *Atmos. Environ.* **1996**, *30*, 3109.
(51) Reisinger, A. R. *Atmos. Environ.* **2000**, *34*, 3865.
(52) Marinoni, A.; Laj, P.; Sellegri, K.; Mailhot, G. *Atmos. Chem. Phys.* **2004**, *4*, 715.
(53) Amoroso, A.; et al. *Water, Air, Soil Pollut.* **2008**, *188*, 81.
(54) Acker, K.; et al. *Geophys. Res. Lett.* **2006**, *33*, DOI: 10.1029/2005GL024643.
(55) Stemmler, K.; Vlasenko, A.; Guimbaud, C.; Ammann, M. *Atmos. Chem. Phys.* **2008**, *8*, 5127.
(56) Donaldson, D. J.; Vaida, V. *Chem. Rev.* **2006**, *106*, 1445.
(57) Stutz, J.; et al. *J. Geophys. Res., [Atmos.]* **2004**, *109*, DOI: 10.1029/2003JD004135.
(58) Andrés-Hernandez, M. D.; Notholt, J.; Hjorth, J.; Schrems, O. *Atmos. Environ.* **1996**, *30*, 175.
(59) Stemmler, K.; et al. *Atmos. Chem. Phys.* **2007**, *7*, 4237.
(60) Bröske, R.; Kleffmann, J.; Wiesen, P. *Atmos. Chem. Phys.* **2003**, *3*, 469.
(61) Stemmler, K.; et al. *Nature (London)* **2006**, *440*, 195.
(62) Kurtenbach, R.; et al. *Atmos. Environ.* **2001**, *35*, 3385.
(63) Li, S. P.; Matthews, J.; Sinha, A. *Science* **2008**, *319*, 1657.

JP900685F